Acta Pharmaceutica Sinica B 2022;12(10):3877−3890

Chinese Pharmaceutical Association
Institute of Materia Medica, Chinese Academy of Medical Sciences

Acta Pharmaceutica Sinica B

www.elsevier.com/locate/apsb
www.sciencedirect.com

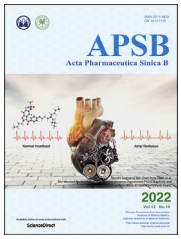

ORIGINAL ARTICLE

Gli1 promotes epithelial−mesenchymal transition and metastasis of non-small cell lung carcinoma by regulating snail transcriptional activity and stability

Xueping Lei[a,b,†], Zhan Li[a,†], Yihang Zhong[a,†], Songpei Li[a], Jiacong Chen[a], Yuanyu Ke[a], Sha Lv[a], Lijuan Huang[a], Qianrong Pan[a], Lixin Zhao[a], Xiangyu Yang[a], Zisheng Chen[b,*], Qiudi Deng[c,*], Xiyong Yu[a,*]

[a]*Guangzhou Municipal and Guangdong Provincial Key Laboratory of Molecular Target & Clinical Pharmacology, the NMPA and State Key Laboratory of Respiratory Disease, School of Pharmaceutical Sciences and the Fifth Affiliated Hospital, Guangzhou Medical University, Guangzhou 511436, China*
[b]*Department of Respiratory and Critical Care Medicine, the Sixth Affiliated Hospital of Guangzhou Medical University, Qingyuan People's Hospital, Qingyuan 511518, China*
[c]*GMU-GIBH Joint School of Life Sciences, Guangzhou Medical University, Guangzhou 511436, China*

Received 9 December 2021; received in revised form 18 February 2022; accepted 31 March 2022

KEY WORDS

Non-small cell lung carcinoma;
Metastasis;
Epithelial−mesenchymal transition;
Glioma-associated oncogene 1;
Promote;
Snail;
Protein stability;

Abstract Metastasis is crucial for the mortality of non-small cell lung carcinoma (NSCLC) patients. The epithelial−mesenchymal transition (EMT) plays a critical role in regulating tumor metastasis. Glioma-associated oncogene 1 (Gli1) is aberrantly active in a series of tumor tissues. However, the molecular regulatory relationships between Gli1 and NSCLC metastasis have not yet been identified. Herein, we reported Gli1 promoted NSCLC metastasis. High Gli1 expression was associated with poor survival of NSCLC patients. Ectopic expression of Gli1 in low metastatic A549 and NCI-H460 cells enhanced their migration, invasion abilities and facilitated EMT process, whereas knock-down of Gli1 in high metastatic NCI-H1299 and NCI-H1703 cells showed an opposite effect. Notably, Gli1 overexpression accelerated the lung and liver metastasis of NSCLC in the intravenously injected metastasis model. Further research showed that Gli1 positively regulated Snail expression by binding to its promoter and enhancing

*Corresponding authors. Tel.: +86 20 37103261 (Xiyong Yu); +86 20 31100902 (Qiudi Deng); +86 76 36411049 (Zisheng Chen).
E-mail addresses: yuxycn@gzhmu.edu.cn (Xiyong Yu), dengqiudi@gzhmu.edu.cn (Qiudi Deng), 502463784@qq.com (Zisheng Chen).
[†]These authors made equal contributions to this work.
Peer review under responsibility of Chinese Pharmaceutical Association and Institute of Materia Medica, Chinese Academy of Medical Sciences

https://doi.org/10.1016/j.apsb.2022.05.024

GANT-61

its protein stability, thereby facilitating the migration, invasion and EMT of NSCLC. In addition, administration of GANT-61, a Gli1 inhibitor, obviously suppressed the metastasis of NSCLC. Collectively, our study reveals that Gli1 is a critical regulator for NSCLC metastasis and suggests that targeting Gli1 is a prospective therapy strategy for metastatic NSCLC.

1. Introduction

Non-small cell lung cancer (NSCLC), including adenocarcinoma (LUAC), lung squamous cell carcinoma (LUSC) and large cell carcinoma subtypes, is characteristic with high incidence and poor survival rate[1]. The overall survival of NSCLC patient was 10%−20% or less, with a median survival of 8−10 months. Metastasis is the leading cause for NSCLC-related mortality. Approximately 75% NSCLC patients show evidences of local or distant metastasis, and only about 15% metastatic NSCLC patient survive for five or more years after diagnosis. NSCLC can spread to local or distant organs, including lung, liver, brain and bone, either individually or simultaneously[2,3]. Most of NSCLC patients already have distant metastasis when they were diagnosed, which severely increase the difficulty of therapy and reduces patient survival. And the molecular mechanisms underlying these processes remain largely unknown. Therefore, it is urgent to reveal the underlying mechanism and identify effective therapeutic targets or prognostic biomarkers for metastatic NSCLC[4,5].

NSCLC metastasis is a complex multi-step cell biological process that involves in serial cascade events, including acquisition of mesenchymal cells abilities, dissociation from the primary tumor and intravasate the endothelium to turn into circulating tumor cells, surviving circulating tumor cells extravasate into the parenchyma, adhesion, and colonization at the target site[3,6]. Growing evidences illustrate that epithelial−mesenchymal transition (EMT), a process during which epithelial cells lose their apical-basal polarity and then adopt a mesenchymal phenotype, plays a key role in tumor metastasis. EMT contributes to several processes of tumor metastasis, including cancer cells shed from the primary tumor, intravasate into and survive in circulation, and extravasate into the distant organ[7−9]. EMT also involves in the stemness and chemoresistance of many cancer cells[10]. During EMT, the level of epithelial markers (*e.g.*, E-cadherin and ZO1) was decreased, whereas the level of mesenchymal markers (*e.g.*, Vimentin, N-cadherin and Fibronectin) was increased. High N-cadherin, Vimentin and low E-cadherin level in tumor tissues often predict poor overall survival of patient[11]. And reversing EMT process using certain chemotherapeutic agents or genetic deletion has been demonstrated to attenuate the process of NSCLC metastasis. Snail is one of most important EMT-inducing transcriptions factors, and has been demonstrated to activate EMT process in multiple epithelial cancer cell lines and primary tumor[7,12]. All these suggest that EMT is crucial for NSCLC metastasis, although the precise mechanisms are still unclear[13,14].

Hedgehog/Glioma-associated oncogene (Hh/Gli) signaling pathway is frequently activated in several types of tumor tissues, including breast cancer, colorectal carcinoma, gastric cancer and osteosarcoma[15−17]. Gli1 is a critical effector of Hh/Gli1 signaling pathway and it initiates tumor progress by continuous transactivation of target gene such as Hh, Gli1, protein patched homolog 1 (PTCH1), smoothened (SMO). Gli1 is aberrantly active in many tumor tissues *via* upstream PTCH/SMO-dependent (classical) or PTCH/SMO-independent (non-classical) signaling pathway[18,19]. Gli1 overexpression is associated with the self-renewing phenotype of cancer stem cell, drug resistance and aggressive behavior[20]. Recently, several studies revealed that Hh/Gli1 was critical for NSCLC tumorigenesis and maintenance. Gli1 expression was increased in adenocarcinomas and squamous cell carcinomas. And high Gli1 expression may associate with aggressive behavior of lung cancer[21,22]. Moreover, Gli1 expression in lung cancer tissues was thought to correlate with the expression of EMT marker. However, the role of Gli1 in NSCLC metastasis and the underlying mechanism remain unclear[23].

In this study, we showed that Gli1 level was up-regulated in NSCLC tissues and high Gli1 expression indicated poor overall survival of NSCLC patients. Gli1 enhanced the invasion and metastasis of NSCLC *in vitro* and *in vivo*. Mechanistically, we found that Snail was crucial for Gli1-mediated enhancement on the invasion and EMT of NSCLC. And Gli1 positively regulated Snail expression by binding to its promoter and enhancing its protein stability. Furthermore, targeting Gli1 with GANT-61 significantly suppressed the metastasis of NSCLC. Taken together, our study provides strong evidences that Gli1 is a facilitator of NSCLC metastasis and illustrates the underlying molecular mechanism. Our study suggests that Gli1 might be developed into a potential therapeutic target for NSCLC metastasis.

2. Material and methods

2.1. Reagents and antibodies

Gli1 antibody (AF3455) was purchased from R&D Systems Inc (Minneapolis, MN, USA). EMT antibody sampler kit (#9782) (including N-cadherin, Vimentin, Snail, E-cadherin, and ZO-1), HRP-conjugated anti-rabbit IgG antibody (#7074), glycogen synthase kinase 3β (GSK-3β) antibody (#12456), and phospho-GSK-3β (Ser9) antibody (#9336) were acquired from cell signaling technology (Danvers, MA, USA). Alexa Fluor 594-conjugated donkey anti-rabbit IgG (ab150064) and Alexa Fluor 488 donkey anti-rabbit IgG (ab150073) were obtained from Abcam (Cambridge, UK). Lipofectamine 3000 and Opti-MEM were products of Invitrogen (Thermo Fisher Scientific, Waltham, MA, USA). ChIP PCR kit was a product of Merck Millipore (Billerica, MA, USA). Dual luciferase reporter gene assay kit was obtained from Promega (Madison, WI, USA). Wide type and mutational Snail vector and siRNA were purchased from Qingke biotech (Wuhan, China). GANT-61, cycloheximide (CHX), MG132 and LiCl were obtained from Shanghai Pottery Biotechnology (Shanghai, China) and dissolved in dimethyl sulfoxide.

Matrigel was obtained from BD Biosciences (Franklin Lakes, NJ, USA). D-Luciferin was obtained from Yeasen (Shanghai, China). Other agents were purchased from Sigma−Aldrich (St Louis, MO, USA).

2.2. Patient species and immunohistochemical (IHC) staining

All human NSCLC tissues were collected from patients who were diagnosed as NSCLC in the Sixth Affiliated Hospital of Guangzhou Medical University. The clinical specimens used in this study were empowered by Institutional Review Board accord with the principles of the Declaration of Helsinki. And written informed consent was received from individual participants prior to sample collection. The paraffin-embedded tissue microarrays, containing 90 pairs NSCLC/adjacent non-carcinoma samples were constructed by Shanghai Xinchao Biotech (Shanghai, China). IHC was performed according to a standard protocol. Paraffin-embedded samples were sectioned at 4-μm thickness and applied to standard protocol for deparaffinization and rehydration. After antigens retrieval, the sections were blocked by 1% bovine serum albumin and incubated with Gli1 antibody (1:200) at 4 °C overnight. Subsequently, the sections were washed with PBS and incubated with HRP-conjugated secondary antibody, and then visualized by DAB and counterstained by hematoxylin. Five representative fields of a section were observed and captured with a Carl Zeiss fluorescence microscope. The expression of Gli1 level was scored semiquantitatively using the immunoreactive score as previous described[24].

2.3. Cell lines and cell culture

Human NSCLC cell lines including NCI-H1299, NCI-H292, NCI-H460, NCI-H1975, NCI-H1703, NCI-H358, NCI-H1650 and A549, and HEK-293 T cells were obtained from American Type Culture Collection. All the NSCLC cells were cultured in RPMI/1640 medium (Gibco) supplemented with 10% fetal bovine serum and maintained in humidified atmosphere at 37 °C with 5% CO_2. As for the HEK-293 T cells were cultured in DMEM (Gibco). STR Multi-Amplification Kit was used to confirm that all cells have no cross contamination with other cell lines.

2.4. Establishment of Gli1 stably transfected cell lines

The Gli1 knock-down and overexpressing lentivirus were packaged and purified by GenePharma (Suzhou, China). The cells were transfected with lentiviral vectors including LV3-NC (control for the over expression group), LV3-Gli1-homo-3216 (Gli1 over-expression), LV5 (control for the knock-down group) and Gli1-shRNA (Gli1 knockdown group) in the presence of polybrene (10 μg/μL). After 48 h, cells were selected by puromycin (4 μg/mL) for 7 days to acquire the Gli1 stably knock-down or overexpressing cells. RT-qPCR assay and Western blotting assay were conducted to confirm the gene silencing or overexpression. The targeting sequence of Gli1 shRNA is 5′-GCAGUAAAGCCUU-CAGCAAUG-3′.

2.5. Wound healing assay

The NSCLC cells were seeded in 6-well plate at a density of 5×10^5 cells per well and cultured until it reached approximately 100% confluence. The cells were starved with serum-free RPMI/1640 medium for 6 h, and then the wound was created across the monolayer using 20 μL pipette tip. The cells were incubated for another 24 h and cell migration was ascertained by photography at the same filed. The cells migrated to the scraped area were analyzed using Image-Pro Plus 6.0 software (Media Cybernetics, Rockville, MD, USA).

2.6. Transwell migration and invasion assay

The Transwell migration and invasion assay were performed with Transwell pore polycarbonate membrane insert (8 μm) with or without Matrigel-coated invasion chambers, respectively. Briefly, the cells were suspended in serum-free medium and seeded into the upper chamber at the density of 2×10^4 cells/well, and the lower chamber were filled with 600 μL fresh complete medium. After incubating for 24 h, the cells that adhered to the lower surface were fixed using paraformaldehyde. The migrated or invaded cells were captured with a microscope and analyzed using Image-Pro Plus 6.0 software after being stained with 0.1% crystal violet.

2.7. RNA extraction and quantitative real-time polymerase chain reaction (RT-qPCR)

Total RNA Extraction Kit (Solarbio Science & Technology, Beijing, China) was used to isolate total RNA in accordance with the manufacturer's protocol. Total RNA was reverse-transcribed into complementary DNA (cDNA) using SuperScript VILO cDNA Synthesis Kit (Invitrogen). The reaction solution contains primers, TB Green Premix Ex Taq II (TaKaRa, Japan) and cDNA templates. The qPCR analysis was conducted with LightCycler 480 Real-Time PCR System (Roche, Swiss). The conditions of cycling parameters were as follow: 45 cycles of 95 °C for 10 s, 60 °C for 20 s and 72 °C for 20 s.

All genes were analyzed in triplicate, and relative expression was normalized to house-keeping gene GAPDH. The primers used in RT-qPCR assay are showed in Supporting Information Table S1.

2.8. Immunofluorescence assay

For immunofluorescence assay, the cells grown on the 15-mm cover glass were fixed with 4% paraformaldehyde for 30 min at room temperature, permeabilized with Triton X-100 for 5 min and then blocked with 5% bovine serum albumin for 1 h. After that, the cells were incubated with the primary antibody overnight at 4 °C. The proteins were visualized by incubating with secondary antibody conjugated to Alexa Fluor 594 for 1 h at room temperature. The nuclear was recognized with DAPI staining. The images were captured with LSM 880 laser scanning confocal microscope (Zeiss, Oberkochen, Germany). And the quantitative analysis of immunofluorescence was using Image-Pro-Plus 6.0.

2.9. Western blotting assay

The cells were harvested and lysed using ice-cold RIPA buffer containing protease (BD Biosciences). BCA Protein Assay Kit (Beyotime) was applied to detect protein concentration, and equal amounts (40 μg) of protein were separated through SDS-PAGE and transferred onto polyvinylidene difluoride membranes. And then the blots were visualized through immunoblotting with indicated antibodies. The membranes were probed with primary antibody overnight at 4 °C and incubated with HRP-labeled secondary antibody 1 h at room temperature, and then visualized ECL

chemiluminescence system (Bio-Rad). Finally, the blots were scanned and analyzed using Amersham Imager 600 (GE, Boston, USA).

2.10. *Snail protein half-life assay*

To estimate the half-life of Snail protein in different cells, CHX pulse-chase experiments were conducted as previously described[25]. In brief, the cells were seeded at 6-well plates and cultured overnight. The cells were treated with 2 μmol/L CHX for 0, 0.5, 1, 2, 4 and 6 h. After that, the cells were collected and lysed using ice-cold RIPA buffer and Western blotting assay was conducted to detect Snail expression. Quantitative data based on densitometry was acquired using Image-Pro Plus 6.0 software (NIH, NY, USA).

2.11. In vivo *metastasis assay*

Five-week-old Male BABL/c (*nu/nu*) mice were obtained from Hua Fukang Experimental Animal Center (Beijing, China). All the experiments involved in animals were performed according to the Laboratory Animal Ethics Committee of Guangzhou Medical University. The cells were collected and suspended in ice-cold PBS. And the cells were injected into the tail with 4×10^6 cells each mice. Metastatic lesions were monitored with bioluminescence imaging at sixth week. Briefly, the mice were anaesthetized with pentobarbital sodium and intraperitoneally injected with 150 mg/kg D-luciferin. The bioluminescence was captured using an IVIS Lumina XRMS Series III (PerkinElmer, Alameda, CA, USA) and analyzed using Living Image Software 4.3.1. And then the mice were sacrificed and the lung and liver were harvested for further H&E assay. As for the anti-metastatic effect of GANT-61 *in vivo*, NCI-H1299^{Luc} cells were injected into the tail veins of mice with 4×10^6 cells per mice. 15 days later, the mice were intraperitoneal injected with 50 mg/kg GANT-61 every two days for totally 30 days. And then the mice (10 mice in each group) were subjected to the bioluminescence assay.

2.12. *Transient transfection of plasmid and small interfering RNA (siRNA)*

The plasmid and siRNA duplexes of Snail were supplied by Qingke Biotechnology (Beijing, China). Cells were seeded into 6-well plate and grown to 50%−60% confluence, and then the cells were transfected with the plasmid and siRNA using Lipofectamine 3000 following the standard procedure. And the transfection efficacy was determined with RT-qPCR and Western blotting assay after indicated time. The targeting sequences of Snail siRNA is 5′-CCCACUCAGAUGUCAAGAA-3′.

2.13. *Luciferase reporter assay*

The HEK-293 T cells were seeded in 24-well plates and cultured overnight, and then the cells were transfected with pGL3-Snail-promoter^{WT}-Luc, pGL3-Snail-promoter^{Mut1}-Luc, and pGL3-Snail-promoter^{Mut2}-Luc using Lipofectamine 3000, respectively. And *Renilla* luciferase promoter was transfected at the same time. After 48 h, the firefly and *Renilla* luciferase activities were analyzed with dual-luciferase assay kit following with the standard procedure. *Firefly* luciferase was normalized to the internal *Renilla* luciferase control to investigate the reporter translation efficiency.

2.14. *Chromatin immunoprecipitation (ChIP) assay*

The ChIP assay was performed as previous described with some adaption[26]. Briefly, the cells were cross-linked with 1% formaldehyde solution and glycine solution was used to terminate the reaction. The cells were collected and lysed, and nucleoprotein complexs were sonicated for 10 cycles (1 cycle; 10 s on, 30 s off) using a sonicate conductor at an intensity of 200 W. Then, the anti-Gli1 and anti-IgG were coupled with Dynabeads protein A/G at 4 °C for 1 h, and then added and incubated with the complexes overnight at 4 °C. After that, Protein A/G magnetic beads were added to precipitate the indicated fragments for another 4 h at 4 °C. After that, indicated DNA was purified with DNA purification magnetic beads and eluted with DNA elution buffer. Semiquantitative PCR was conducted to recognize the region interacting with the Gli1 specific primers listed in Supporting Information Table S2. The amount of immunoprecipitated DNA was normalized to the input.

2.15. *Statistical analysis*

Data are presented as mean ± standard deviation (SD) of three independent experiments and statistical analyses were conducted with GraphPad Prism 7 (GraphPad, San Diego, CA, USA). Unpaired student's *t* test was used to determine statistical significance between two groups, and one-way analysis of variance (ANOVA) was used to evaluate statistical significance among three or more groups. $P < 0.05$ was considered to indicate statistical significance. The correlation between Gli1 and Snail expression in tumor tissues was analyzed by Pearson's correlation coefficients.

3. Results

3.1. *High-level of Gli1 expression in NSCLC tissues is associated with metastasis and poor survival*

To gain insight into the role of Gli1 in NSCLC, we first detected Gli1 level in paraffin-embedded tissue microarrays containing 90-paired normal lung tissues and NSCLC tissues using immunohistochemistry (IHC) assay. The results show that Gli1 level was obviously higher in tumor tissues than the pair-matched normal tissues (Fig. 1A and B and Supporting Information Fig. S1). Gli1 overexpression was further confirmed in representative 16-paired NSCLC tissues and normal tissues using RT-qPCR assay. And Gli1 mRNA was significantly increased in tumor tissues than the adjacent lung tissues (Fig. 1C). We further analyzed the relationship between Gli1 level and clinical parameters of NSCLC patients. We did not observe any significant difference in Gli1 expression based on sex or age. And Gli1 expression was significantly positively correlated with T stage and TNM stage of NSCLC patient (Fig. 1D and Supporting Information Table S3). Kaplan−Meier analysis indicated that patient with high Gli1 level showed a shorter overall survival than those with low Gli1 expression (Fig. 1E). GEPIA database showed that Gli1 was up-regulated in the tumor tissues of LUSC patients. And LUAD patients with high Gli1 level had a poor prognosis (Fig. 1F and G). We also detected Gli1 expression in a series of NSCLC cell lines by Western blotting assay, and then investigated their migration abilities using Transwell migration assay. The results show that Gli1 expression might positively correlate with the migration ability of NSCLC cells. NCI-H1299 and NCI-H1703 with relatively high Gli1 level had better migration

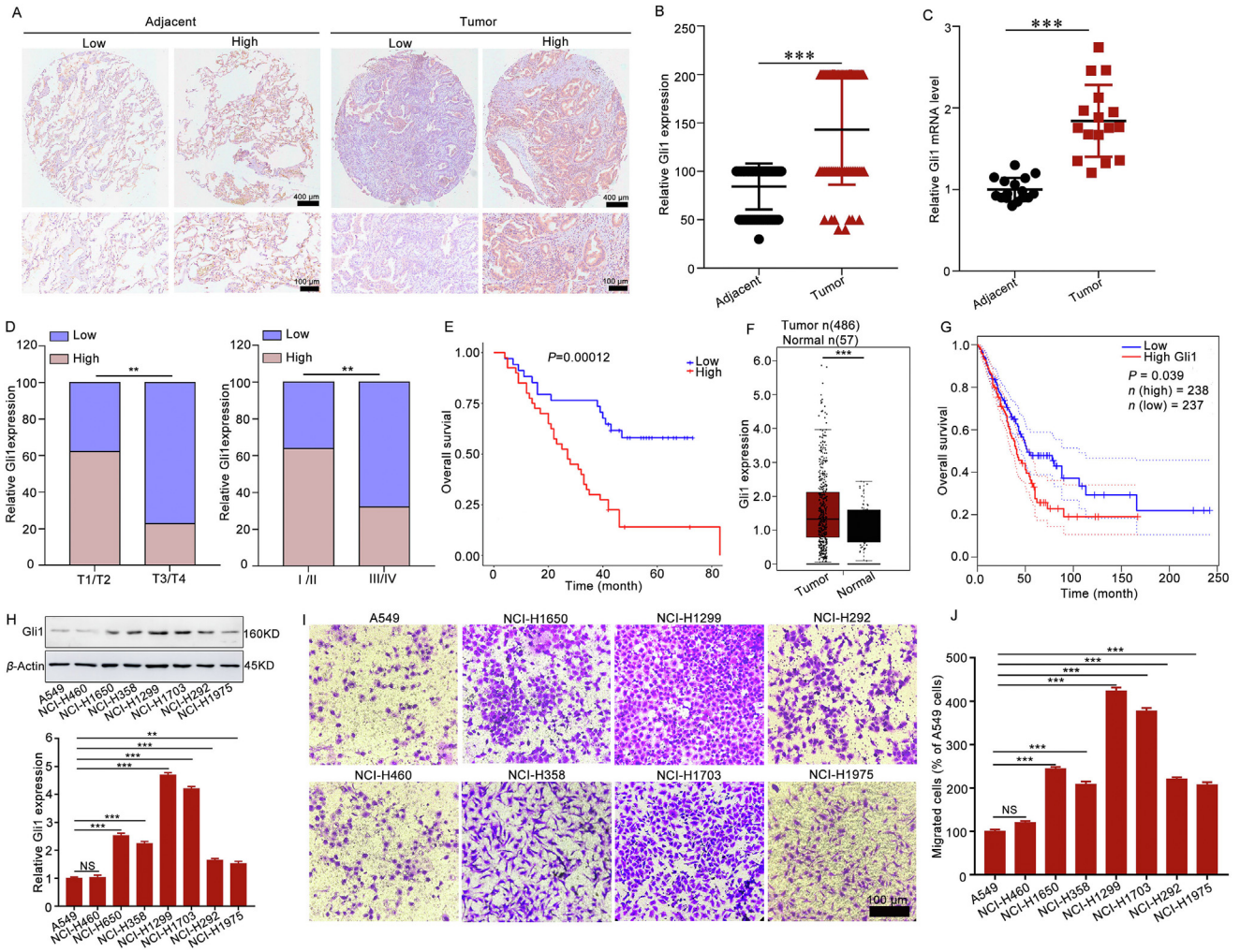

Figure 1 Gli1 is up-regulated in NSCLC tissues and Gli1 overexpression indicates poor survival of NSCLC patients. (A, B) The Gli1 level in NSCLC tissues and matched normal tissues was detected by IHC assay. The representative images were presented in (A) and the statistical data were showed in (B), $n = 90$, $^{***}P < 0.001$ *vs*. adjacent tissues. (C) RT-qPCR assay detected Gli1 mRNA level in representative 16-paired NSCLC tissues and normal tissues, $n = 16$, $^{***}P < 0.001$ *vs*. adjacent tissues. (D) High Gli1 expression is relevant to clinical outcomes of NSCLC patients, $n = 90$, $^{**}P < 0.01$ *vs*. T1/T2 stage or I/II stage. (E) Kaplan−Meier analysis of the over survival of NSCLC patients, $n = 90$. (F) Gli1 expression in 486 LUSC cases based on GEPIA database, $n = 486$ in tumor tissues group, $n = 57$ in normal tissues group. (G) Kaplan−Meier analysis of the over survival of LUAC patient based on GEPIA database. $^{***}P < 0.001$ *vs*. normal tissues. (H) The Gli1 level in a serial of NSCLC cell lines detected by Western blotting assay. (I, J) The migration ability of NSCLC cells was evaluated by Transwell migration assay. $n = 3$, $^{**}P < 0.01$; $^{***}P < 0.001$ *vs*. A549 cells in (H) and (J). All the data are showed as mean ± SD.

ability than other cells (Fig. 1H−J). Taken together, these results suggest that high Gli1 level might associate with the clinical outcomes in NSCLC tissues and cells.

3.2. *Enhanced Gli1 expression promotes migration, invasion, EMT*

To identify the function of Gli1 in NSCLC, we stably overexpressed Gli1 using lentiviral vector in low metastatic A549 cells. After confirming its transfection efficiency using Western blotting assay and RT-qPCR assay (Fig. 2A and B), we conducted RNA sequence analyze with $A549^{NC\ vector}$ and $A549^{Gli1\ vector}$ cells. RNA-sequencing analysis revealed that there were 270 genes obviously up-regulated and 224 genes were down-regulated (Supporting Information Fig. S2). KEGG analysis indicated that the up-regulated genes were highly enriched in "cell migration" and "cell mobility". We speculated that Gli1 might correlate with the invasion and metastasis of NSCLC (Fig. 2C). To confirm this hypothesis, Gli1 was overexpressed in another low metastatic NCI-H460 cell, and further verified its transfection efficacy using Western blotting assay and RT-qPCR assay (Supporting Information Fig. S3). Wound healing assay, Transwell migration and invasion assay were performed to elucidate the biological effect of Gli1. In wound healing assay, we found that Gli1 overexpression obviously enhanced the migration ability of A549 cells and NCI-H460 cells (Fig. 2D). Transwell migration and invasion assay also demonstrated that the migrated and invasive abilities of A549 and NCI-H460 cells were significantly enhanced in Gli1 overexpression group (Fig. 2E and F). In order to determine whether Gli1 overexpression promote EMT process, we also detected epithelial and mesenchymal markers of these cells using immunofluorescence assay and Western blotting assay. Immunofluorescence assay showed that Gli1

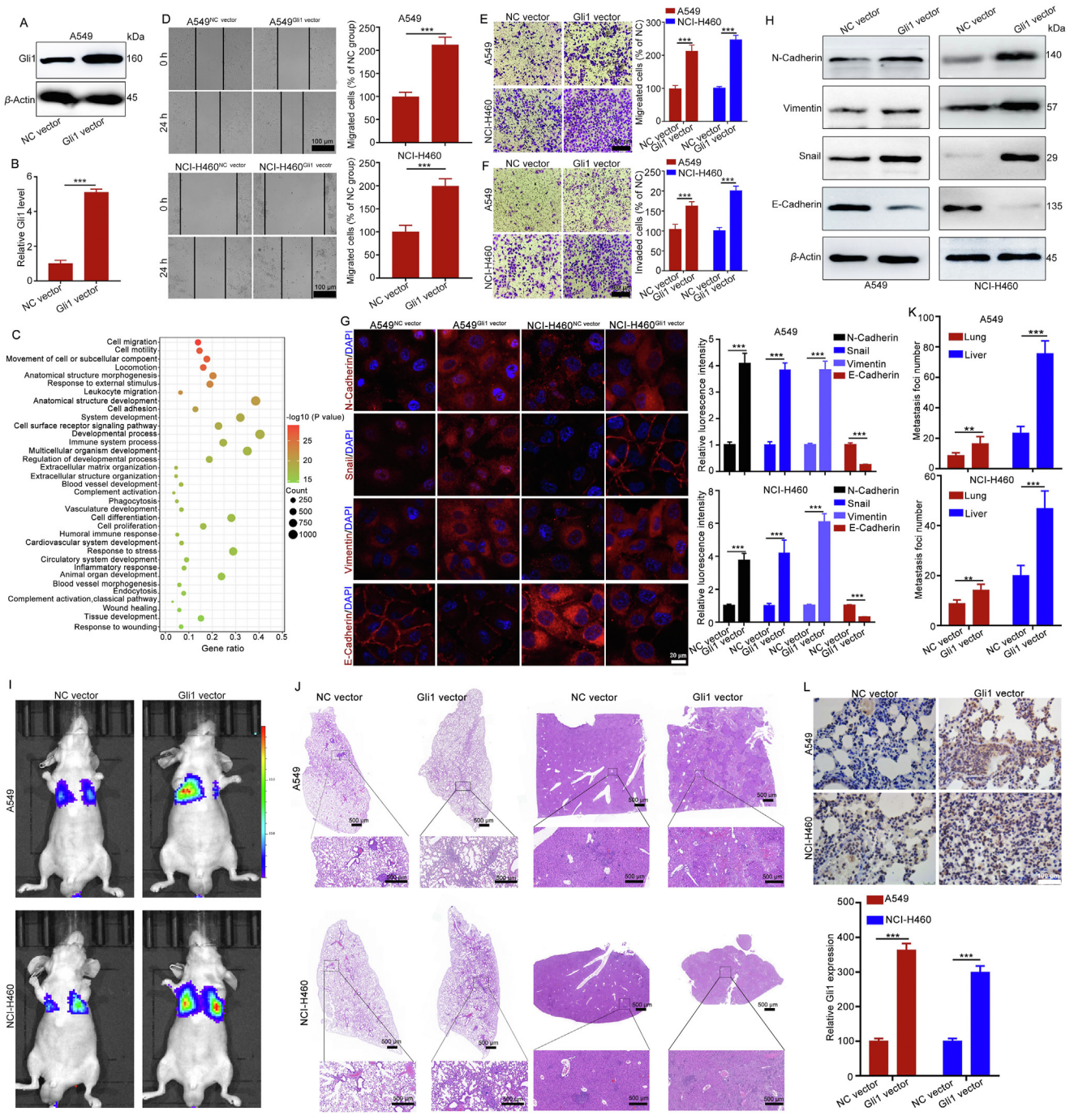

Figure 2 Gli1 promotes migration, invasion, and metastasis of A549 and NCI-H460 cells. (A, B) RT-qPCR and Western blotting assay were subjected to confirm the transfection efficiency. (C) The KEGG analyze of down-regulated genes after Gli1 knockdown. (D) Gli1 overexpression promoted the migration ability of A549 and NCI-H460 cells detected by wound healing assay. (E, F) Gli1 overexpression enhanced the migration and invasion abilities of A549 and NCI-H460 cells indicated by Transwell migration and invasion assay. The representative images are showed in left panel and the quantitative data are presented in right panel. (G, H) Gli1 overexpression induced EMT detected by immunofluorescence assay and Western blotting assay. The representative images of immunofluorescence assay and quantitative data are showed in (G). The results of Western blotting assay are presented in (H). (I−K) Gli1 overexpression enhanced the metastasis of A549 and NCI-H460 cells. BABL/c (*nu*/*nu*) mice were intravenously injected with$A549^{NC\ vector}$/$A549^{Gli1\ vector}$ and $NCI\text{-}H460^{NC\ vector}$/$NCI\text{-}H460^{Gli1\ vector}$ cells. Six week later, IVIS Lumina II was used to detect the metastasis of the mice. And then the mice were sacrificed and applied for H&E staining to detect the nodules in the lung and liver. There were 10 mice in each group. The representative bioluminsescence images are showed in (I). The representative of H&E staining and the quantification of metastastic nodules were presented in (J) and (K). Scar bar: 500 μm. (L) The Gli1 expression in the pulmonary metastasis focuses was detected by IHC assay. Representative images and quantitative data are shown. The data are presented as mean ± SD, $n = 3$ in (A)−(H), $n = 10$ in (I)−(L), $^{***}P < 0.001$ compared with the NC vector group.

overexpression increased the level of mesenchymal marker including N-cadherin, Vimentin, Snail, but reduced E-cadherin (epithelial marker) expression (Fig. 2G). Similar results were observed in Western blotting assay, Gli1 overexpression up-regulated N-cadherin, Vimentin and Snail expression but reduced E-cadherin expression (Fig. 2H). To further appraise the role of Gli1, we established a metastasis model by tail intravenous injected with $A549^{NC\ vector}$/$A549^{Gli1\ vector}$ and $NCI\text{-}H460^{NC\ vector}$/$NCI\text{-}H460^{Gli1\ vector}$ cells. The *in vivo* imaging system showed that mice injected with $A549^{Gli1\ vector}$ or $NCI\text{-}H460^{Gli1\ vector}$ cells have greater bioluminescence in the lung and liver than that injected with $A549^{NC\ vector}$ or $NCI\text{-}H460^{NC\ vector}$ cells (Fig. 2I). We also investigated the lung and liver nodule formation in mice using H&E staining and found that Gli1 overexpression increased the metastatic foci number in the lung and liver (Fig. 2J and K). IHC assay demonstrated that Gli1 expression in pulmonary metastasis focuses of $A549^{Gli1\ vector}$ and $NCI\text{-}H460^{Gli1\ vector}$ group were obviously higher than $A549^{NC\ vector}$ and $NCI\text{-}H460^{NC\ vector}$ group (Fig. 2L). All these results indicate that Gli1 overexpression promoted the migration, invasion, EMT and metastasis of NSCLC.

3.3. *Genetic depletion of Gli1 suppresses the migration, invasion, EMT and metastasis of NSCLC*

Gli1 was also silenced in two high metastatic cells NCI-H1299 and NCI-H1703 cells to confirm its metastatic potential (Fig. 3A and B). As expected, wound healing assay showed that the migrated cells number were reduced in $NCI\text{-}H1299^{shGli1}$ and $NCI\text{-}H1703^{shGli1}$ cells in comparison to the scramble group (Fig. 3C). Similarly, Gli1 depletion also obviously reduced the migrated and invasive cells in the Transwell migration and invasion assay (Fig. 3D and E). And Gli1 ablation down-regulated N-cadherin, Vimentin and Snail expression but up-regulated E-cadherin expression in immunofluorescence assay and Western blotting assay (Fig. 3F and G), indicating Gli1 ablation attenuated the EMT process. The results of bioluminescence imaging show that Gli1 depletion obviously suppressed lung and liver nodule formation (Fig. 3H). H&E staining indicated that $NCI\text{-}H1299^{shGli1}$ and $NCI\text{-}H1703^{shGli1}$ group displayed a lower average number of lung and liver nodules when compared with $NCI\text{-}H1299^{shNC}$ and $NCI\text{-}H1703^{shNC}$ group (Fig. 3I and J). IHC assay showed Gli1 expression was reduced in $NCI\text{-}H1299^{shGli1}$ and $NCI\text{-}H1703^{shGli1}$ group in comparison to $NCI\text{-}H1299^{shNC}$ and $NCI\text{-}H1703^{shNC}$ group (Fig. 3K). These results suggest that Gli1 may be a potential driver of the metastasis of NSCLC.

3.4. *Snail is necessary and sufficient for Gli1-asscociated EMT and metastasis of NSCLC*

Considering that Snail is one of the most obviously up-regulated genes among EMT markers, and a series of different expression genes such as E-cadherin, Vimentin and MMP11 were also correlated with Snail (Supporting Information Table S4), we speculated Snail might be a critical downstream effector of Gli1. To verify this hypothesis, we overexpressed Snail in $NCI\text{-}H1299^{shGli1}$ and $NCI\text{-}H1703^{shGli1}$ cells by transfected Snail vector and confirmed the transfection efficacy by RT-qPCR and Western blotting assay (Fig. 4A and B). And then wound healing assay, Transwell migration and invasion assay were carried to investigate the migratory and invasive ability of these cells. The result shows that Snail overexpression significantly rescued the migratory and invasive abilities of $NCI\text{-}H1299^{shGli1}$ and $NCI\text{-}H1703^{shGli1}$ cells. The migratory and invaded cell number of $NCI\text{-}H1299^{shGli1}$ and $NCI\text{-}H1703^{shGli1}$ cells transfected with Snail vector were obviously increased compared to the cells transfected with NC vector (Fig. 4C−E). Moreover, we also found that Snail overexpression rescued the downregulation of N-cadherin, Vimentin in $NCI\text{-}H1299^{shGli1}$ and $NCI\text{-}H703^{shGli1}$ cells, but increased ZO1 and E-Cadherin expression (Fig. 4F). We also transfected $A549^{Gli1}$ and $NCI\text{-}H460^{Gli1}$ cells with siRNA Snail and then evaluated their migration, invasion abilities and detected EMT marker expression (Fig. 4G and H). We found that Snail siRNA transfection significantly weakened the migration and invasion abilities of $A549^{Gli1\ vector}$ and $NCI\text{-}H460^{Gli1\ vector}$ cells. Both the number of migration and invasion cells was decreased in $A549^{Gli1vector}$ and $NCI\text{-}H460^{Gli1vector}$ cells transfected with siRNA Snail in comparison with that transfect with siRNA NC (Fig. 4I−K). Snail siRNA also reduced the level of N-cadherin, Vimentin, increased ZO1 and E-cadherin expression in $A549^{Gli1\ vector}$ and $NCI\text{-}H460^{Gli1vecotr}$ cells (Fig. 4L). We also found that Snail overexpression obviously attenuated shGli1-mediated inhibitory effect on Snail expression but had negligible effect on Gli1 expression in NCI-H1299 and NCI-H1703 cells. SiSnail transfection significantly reduced the Gli1-medicated enhancement effect on Snail expression but did not affect Gli1 expression in A549 and NCI-H460 cells (Fig. 4M). These results indicate that Snail did not affect Gli1 expression in this study. In addition, RT-qPCR assay proved that Snail level was obviously increased in lung tumor tissues of NSCLC patients in contrasted with that in the parental group (Fig. 4N). The correlation assay showed that Gli1 level was positively correlated with Snail level in NSCLC tissues (Fig. 4O). These results suggest that Gli1 facilitated the migration, invasion and EMT of NSCLC partly dependent on Snail.

3.5. *Gli1 promotes snail expression by enhancing its transcription activity and protein stability*

Next, we detected Snail protein and mRNA level in several pairs of cells using Western blotting assay and RT-qPCR assay. The results show that Gli1 positively regulated Snail mRNA level. Snail expression was obviously increased in $A549^{Gli1\ vector}$ and $NCI\text{-}H460^{Gli1\ vector}$ cells than $A549^{NC\ vector}$ and $NCI\text{-}H460^{NC\ vector}$ cells. Inversely, Gli1 deletion reduced snail level in NCI-H1299 and NCI-H1703 cells (Fig. 5A). Dual-luciferase reporter gene assay indicated that Gli1 overexpression obviously enhanced Snail reporter activity, implying that Gli1 might impact the transcription of Snail (Fig. 5B). We identified two potential Gli1-binding sites in the promoter region of Snail using the JASPAR database, from −381 to −370 bp and from −42 to −8 bp of the snail promoter (Supporting Information Table S2), and the binding site is 5′-GACCACCCA-3′. We mutated the binding site "1" (to CAGGAGCGG) to generate pGL3-Snail-promoterMut1-Luc and "2" (to CAGGAGCTG) to generate pGL3-Snail-promoterMut2-Luc. And dual-luciferase assay proved that the luciferase activity was obviously reduced in cells transfected with pGL3-Snail-$promoter^{Mut1}$-Luc (P0WT), pGL3-Snail-$promoter^{Mut2}$-Luc (P0M2), and pGL3-Snail-$promoter^{Mut1}$-Luc combined with pGL3-Snail-$promoter^{Mut2}$-Luc (P0M1+M2) when compared with that transfected pGL3-Snail-$promoter^{WT}$-Luc (P0WT) (Fig. 5C). ChIP-qPCR analysis was performed in NCI-H1299 cells by using an anti-Gli1 and anti-IgG antibody. The results show that relative enrichment of Snail promoter in anti-Gli1 group were significant increased than the anti-IgG group (Fig. 5D). All these results suggest that Gli1 regulated Snail mRNA by binding to its promoter. Considering Snail was a highly labile

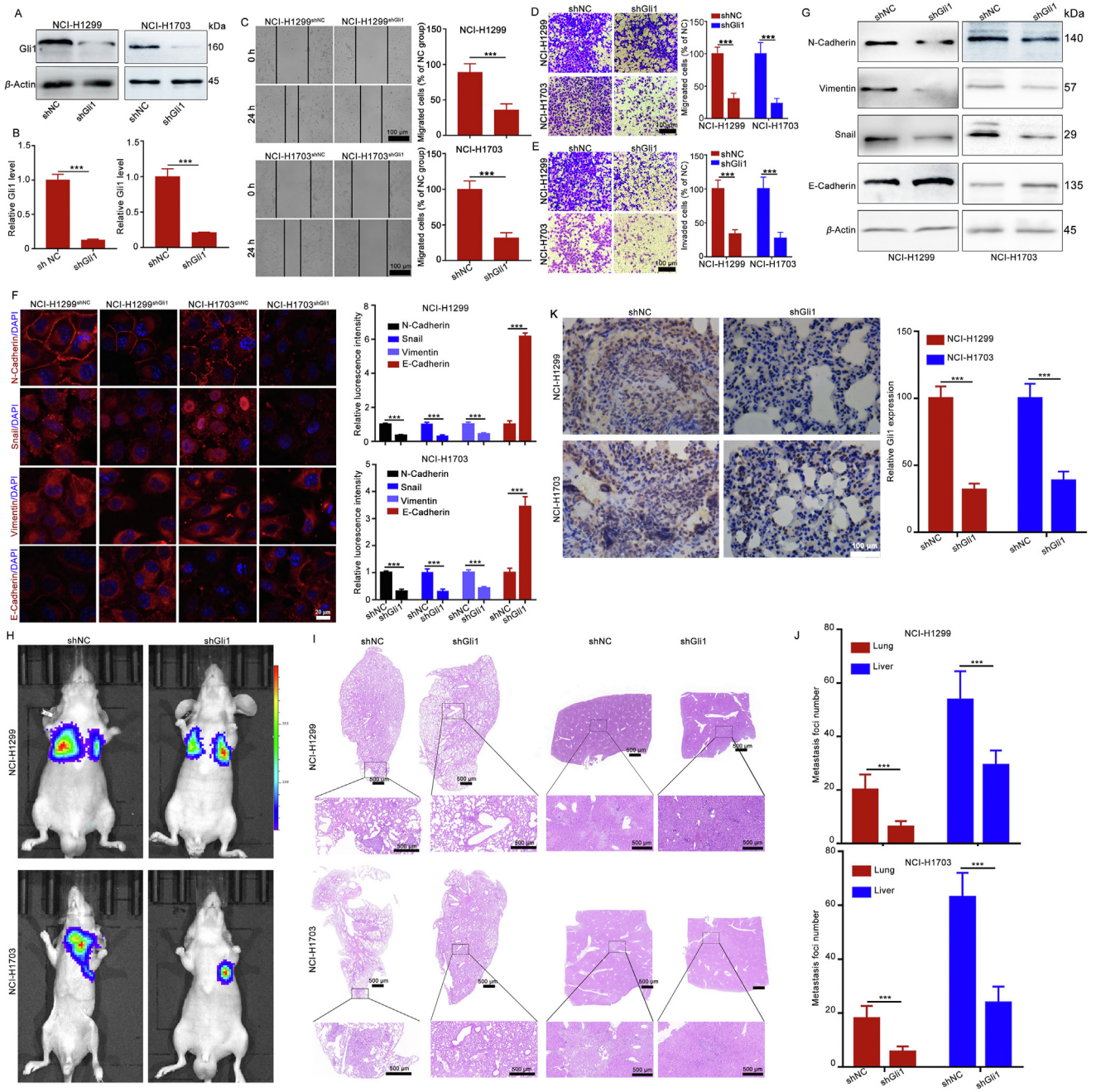

Figure 3 Gli1 silence suppresses migration, invasion and metastasis of NCI-H1299 and NCI-H1703 cells. (A, B) Gli1 shRNA transfection obviously reduced Gli1 level in NCI-H1299 and NCI-H1703 cells detected by RT-qPCR and Western blotting assay. (C) Gli1 knockdown reduced the horizontal migration of NCI-H1299 and NCI-H1703 cells in wound healing assay. (D, E) Gli1 depletion suppressed the migration and invasion abilities of NCI-H1299 and NCI-H1703 cells detected by Transwell migration and invasion assay. (F, G) Gli1 silence inhibited the EMT of NCI-H1299 and NCI-H1703 cells indicated by immunofluorescence assay (F) and Western blotting assay (G). (H−J) Gli1 overexpression enhanced the metastasis of A549 and NCI-H460 cells. The mice were intravenously injected with NCI-H1299^{shNC}/NCI-H1299^{shGli1} and NCI-H1703^{shNC}/NCI-H1703^{shGli1}. Six week later, IVIS Lumina II (H) and H&E staining (I) were applied to detect the nodules in the lung and liver, Scar bar: 500 μm. There were 10 mice in each group. Quantitative data of lung and liver metastases were showed in (J). (K) The Gli1 level in the pulmonary metastasis focuses was detected by IHC assay. Representative images and quantitative data are showed. The data are presented as mean ± SD, n = three in (A)−(G), n = 10 in (H)−(K), ***$P < 0.001$ compared with the shNC group.

protein[27], we also evaluated whether Gli1 affect Snail protein stability. The stable Gli1 overexpression or knock-down cells were stimulated with serum in the presence of CHX, an inhibitor of protein biosynthesis, and then detected Snail expression at different time. The results show that Snail protein rapidly degraded to an undetected level within 4 h in A549$^{NC\ vector}$ and NCI-H460$^{NC\ vector}$ cells, but Snail protein level can be detected at 6 h in A549$^{Gli1\ vector}$ and NCI-H460$^{Gli1\ vector}$ cells. Conversely, we found that Gli1 knock-down accelerated Snail degradation in NCI-H1299 and NCI-1703 cells (Fig. 5E). We also investigated whether Gli1 affected

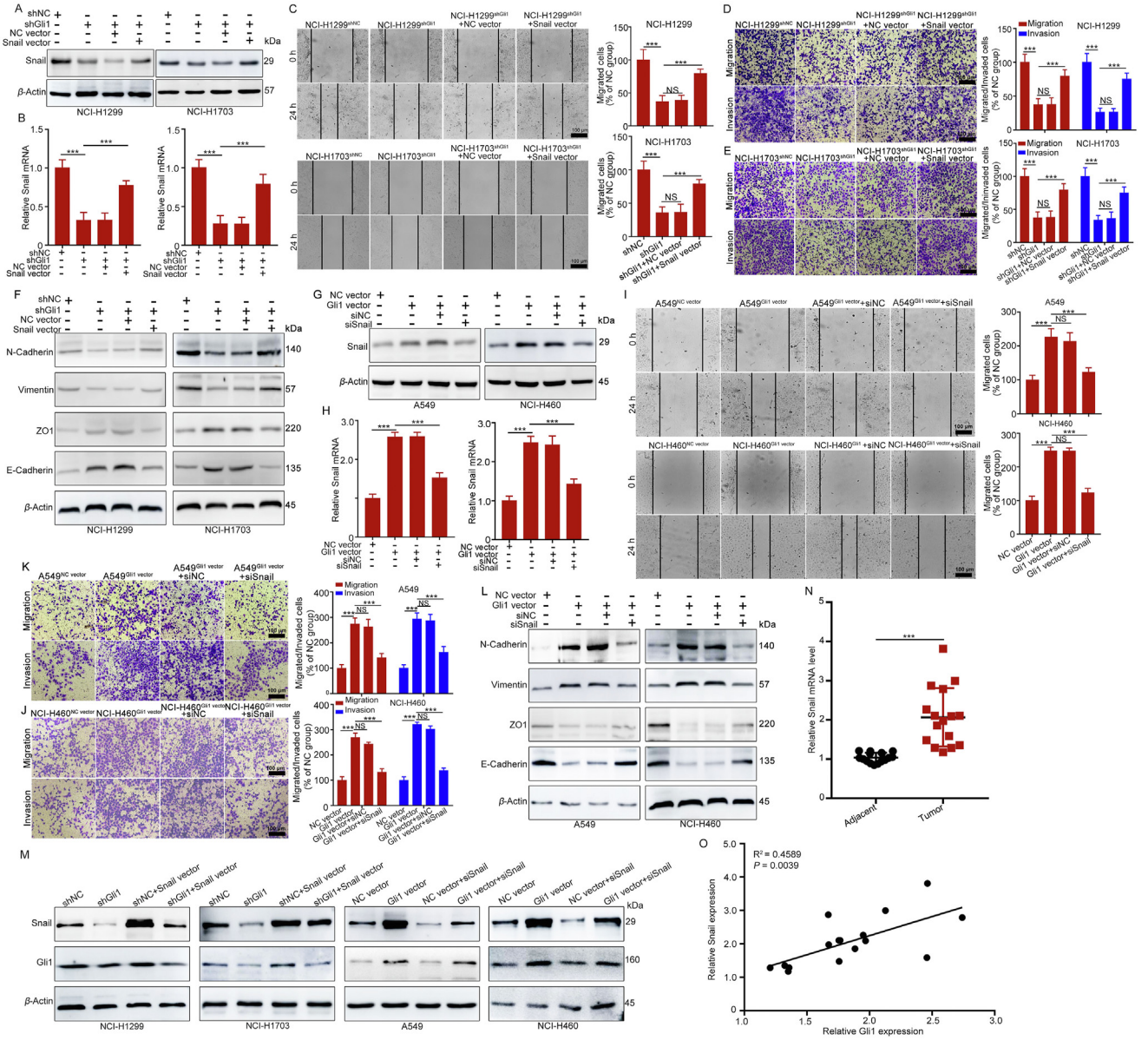

Figure 4 Gli1 promotes the migration, invasion and EMT by regulating Snail. (A, B) NCI-H1299^{shGli1} and NCI-H1703^{shGli1} cells were transfected with NC vector or Snail vector, the transfection efficacy was detected using Western blotting assay (A) and RT-qPCR (B). (C−E) Snail overexpression recovered the migration and invasion abilities of NCI-H1299^{shGli1} and NCI-H1703^{shGli1} cells. NCI-H1299^{shGli1} and NCI-H1703^{shGli1} cells were transfected with NC vector or Snail vector, and then the cells were applied for wound healing assay (C), Transwell migration (D) and invasion assay (E). (F) Snail overexpression reversed EMT process in NCI-H1299^{shGli1} and NCI-H1703^{shGli1}. (G, H) A549$^{Gli1\ vector}$ and NCI-H460$^{Gli1\ vector}$ cells were transfected with siRNA NC or siRNA Snail and then confirmed the transfection efficiency using Western blotting assay (G) and RT-qPCR assay (H). (I−K) Snail silence attenuated the migratory and invasive abilities of A549^{Gli1} and NCI-H460^{Gli1} cells. (L) Snail silence suppressed EMT expression of A549$^{Gli1\ vector}$ and NCI-H460$^{Gli1\ vector}$ cells. (M) Snail overexpression had weak effect on Gli1 expression. The cells transfected with NC vector/Snail vector or siNC/siSnail were subjected for Western blotting assay to detect Snail and Gli1 expression. (N) Snail mRNA level was increased in NSCLC tissues. (O) The correlation relationship of Gli1 and Snail expression NSCLC tissues analyzed with Pearson's correlation coefficients. The data are presented as mean ± SD, n = three in (A)−(M), n = 16 in (N) and (O).

Snail degradation process. We pretreated the NCI-H1299 and NCI-H1703 cells with MG132, a proteasome inhibitor, and found that MG132 abolished GANT-61-mediated inhibitory effect on Snail expression (Fig. 5F). This result suggest that Gli1 might also affect the degradation of Snail. Given that Snail is phosphorylated by GSK-3β and subsequent proteasomal degradation[28,29], thus we detected the level of GSK-3β and its Ser9-phosphorylation, which can auto-inhibit the activity of GSK-3β[28]. We found that Gli1 overexpression decreased GSK-3β expression in A549 and NCI-H460 cells but increased its p-GSK-3β^{Ser9} level. And Gli1 silence had appositive effect on the expression of GSK-3β and p-GSK-3β^{Ser9} in NCI-H1299 and NCI-H1703 cells (Fig. 5 G). Moreover, Gli1 inhibitor GANT-61 significantly reduced Snail level, and LiCl (inhibitor of GSK-3β) obviously attenuated GANT-61 mediated

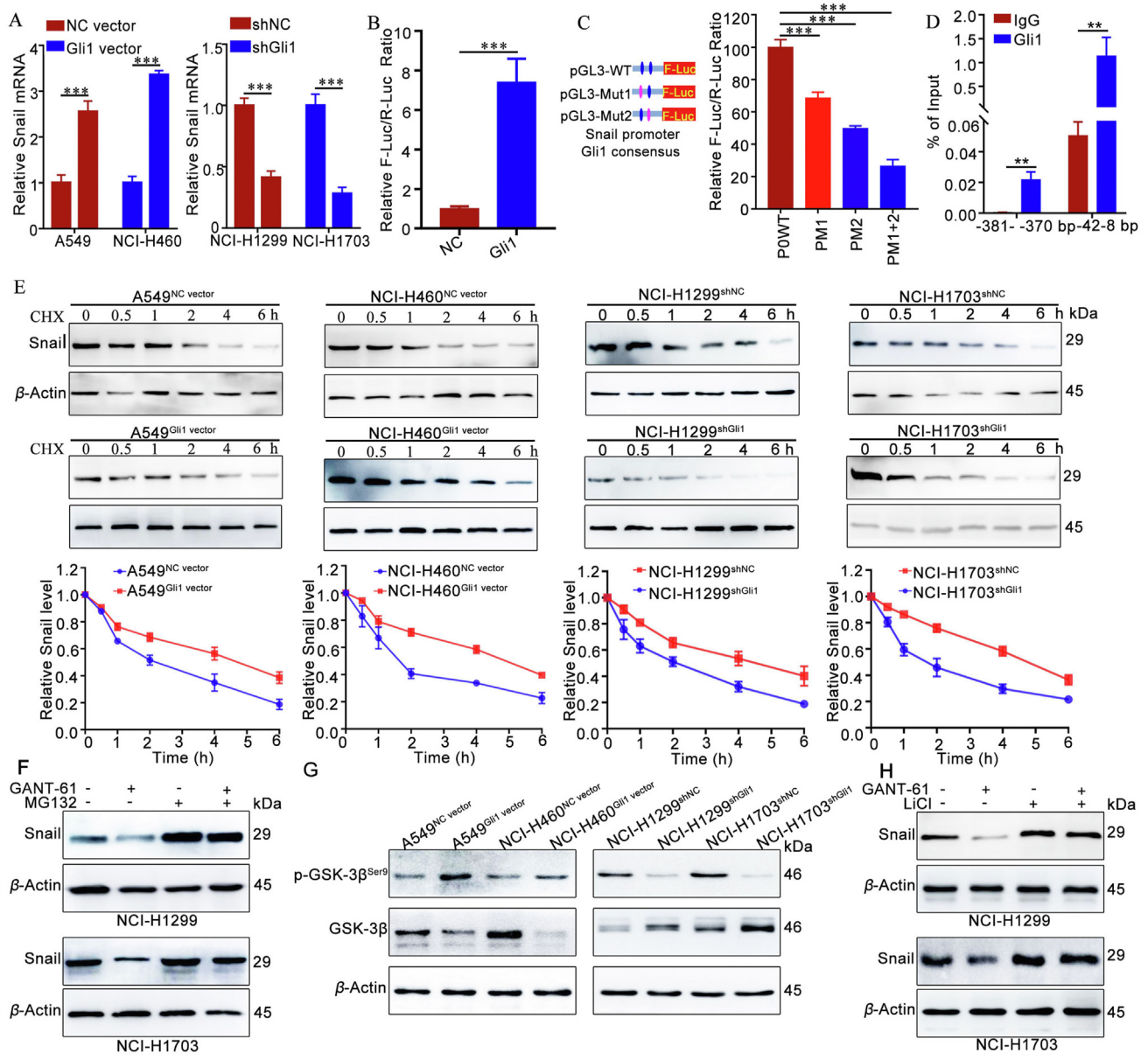

Figure 5 Gli1 regulates Snail by binding to its promoter and enhance its protein stability. (A) Gli1 positively regulated the Snail mRNA level. ***$P < 0.001$ compared with the NC vector or shRNA NC group. (B) Gli1 overexpression significantly increased Snail reporter activity. (C) Dual luciferase reporter assay certificated that Gli1 regulated Snail mRNA by binding to its promoter. ***$P < 0.001$ compared with the wide type group. (D) The result of ChIP-PCR assay. (E) The effect of Gli1 on the protein stability of Snail. The cells were treated with 2 μmol/L CHX for series of periods and subjected to Western blotting assay, and β-actin was set as internal reference. The densitometries of blots were measured with ImageJ software. (F) The effect of Gli1 on the degradation of Snail. The cells were pre-treated with 5 μmol/L MG132 and then treated with GANT-61 for 24 h. After that, the cells were subjected for Western blotting assay to detect Snail expression. (G, H) Gli1 suppressed GSK-3β-dependent Snail degradation. The cells were treated with or without GANT-61 or LiCl, and then subjected for Western blotting assay to detect Snail expression. The level of GSK-3β and p-GSK-3β^{Ser9} expression in a series of cells is shown in (G). The result that LiCL attenuated GANT-61-mediated inhibitory effect on Snail expression is presented in (H). β-Actin was set as loading control. The data are presented as mean ± SD, $n = 3$.

inhibitory effect on Snail (Fig. 5H). All these suggest that Gli1 might enhance Snail protein stability by restraining GSK-3β-mediated Snail degradation. Based on these results, we conclude that Gli1 promoted the EMT and metastasis of NSCLC by directly binding to the promoter of Snail and enhanced its protein stability, and then accelerated the EMT and metastasis of NSCLC.

3.6. Pharmacological inhibition of Gli1 suppresses the migration, invasion and metastasis of NSCLC

Next, we evaluated whether GANT-61 could suppress the metastasis of NSCLC. Wound healing assay demonstrated that GANT-61 (10, 20 and 30 μmol/L, which has on significant effect on the

cell proliferation) obviously inhibited the horizontal migration of NCI-H1299 cells (Fig. 6A and B). Transwell migration and invasion assay also confirmed that GANT-61 treatment caused prominent decrease number of migrated and invaded cells in a dose-dependent manner (Fig. 6C−F). Western blotting and RT-qPCR assay showed that GANT-61 treatment reduced N-cadherin, Vimentin, Snail and Slug expression, increased E-cadherin and ZO1 expression (Fig. 6G and H). For *in vivo* metastasis assay, bioluminescence imaging revealed GANT-61 treatment suppressed the metastatic colonization of NCI-H1299 cells into the lung and liver (Fig. 6I). And H&E staining also showed that after GANT-61 treatment, the metastatic nodes in the lung and liver were obviously reduced (Fig. 6J and K). In addition, GANT-61 treatment also reduced Gli1 level in pulmonary metastasis focuses (Fig. 6L). H&E staining demonstrated that GANTI-61 had negligible effect on the major organs of the mice including liver, heart, spleen and kidney (Supporting Information Fig. S4). Collectively, these data suggest that targeting Gli1 was potential to be a therapeutic strategy for NSCLC metastasis.

4. Discussion

NSCLC is one of the most common malignant tumors and displays high incidence of metastasis. Most of patients were diagnosed at late stages with metastasis, which often leads to the failure of therapy. Still now, the underlying mechanism mediated NSCLC metastasis has not yet been elucidated. Thus, it's urgent to indentify and study novel metastasis driver of NSCLC metastasis[30]. In this study, we identified Gli1 as a novel EMT and metastasis driver of NSCLC, and reveled that Gli1 positively regulated the transcription activity and enhanced Snail protein stability by suppressing GSK-3β-mediated Snail degradation. Further research showed that pharmacological inhibition Gli1 using GANT-61 significantly reversed EMT and suppressed metastasis *in vivo*. Our study provides new insight into the underlying molecular mechanism of metastatic NSCLC and facilitates Gli1 as a novel therapeutic target for metastatic NSCLC.

Hh signaling pathway is active during embryogenesis and plays a crucial role in organogenesis, stem cell maintenance, and the upkeep and repair of adult tissues[12]. As a critical effector of Hh signaling pathway, Gli1 plays multi-functional regulator in multiple cancers including breast cancer, glioblastoma, prostate cancer, and cervical cancer[30]. Accumulating evidences indicated that Gli1 was critical for NSCLC progression. Gli1 was overexpressed in lung squamous cell carcinoma and Gli1 blockade enhanced the anti-tumor effect of PI3K inhibitor[31]. Suppression of Gli1 could inhibit cell proliferation, attenuate stemness and induce apoptosis in LUAC[32]. Our previous study also demonstrated that suppressing Gli1 attenuated tumor growth and angiogenesis in NSCLC[33]. All these suggest that Gli1 is promising to be developed into a therapy target for NSCLC. Recently, Gli1 has been demonstrated to involve in the metastasis of breast cancer and gastric cancer[9,34]. However, whether Gli1 expression is associated with NSCLC metastasis and the underlying mechanism are still unclear. In this study, we recognized Gli1 as a promoter of NSCLC metastasis. Gli1 expression was increased in NSCLC tissues and high Gli1 expression often indicated poor patient survival. Further research manifested that Gli1 enhanced EMT and metastasis of NSCLC by positively regulating the transcription activity and protein stability of Snail. These results provide assertive evidence for the role of Gli1 in NSCLC metastasis and indicate the therapeutic potential of Gli1 for NSCLC metastasis.

Experimental evidences showed that Shh/Gli1 signaling pathway has complicated crosstalk with EMT. The activation of Shh/Gli1 signaling pathway contributed to EMT in gastric cancer, breast cancer and lung cancer[35,36]. EMT cells increased mesenchymal features and aggressive properties of non-EMT cells in partly by non-cell autonomous activation of Gli1 in breast cancer, and Gli1 inhibitor GANT-61 treatment blocks this effect[37]. Gli1 could also induce EMT by inhibiting E-cadherin expression in human esophageal squamous cell cancer[38]. Conversely, Gli1 has been demonstrated to an important positive regulator of epithelial differentiation and RNAi-mediated knock-down of Gli1 promoted EMT in pancreatic cancer cells[39]. And Gli1 expression in lung cancer tissues was inversely correlated with E-cadherin expression, indicating Gli1 may involve in EMT process in lung cancer[35]. However, the underlying mechanism and their correlation in NSCLC remain largely unclear. In the present study, we demonstrate that Gli1 promoted EMT process in NSCLC. Gli1 overexpression enhanced the migration, invasion and EMT of NSCLC cells, genetic depletion and pharmacological inhibition of Gli1 attenuated the migration, invasion abilities of NSCLC cells and reversed its EMT process. Further research revealed that Gli1 promoted EMT in a Snail-dependent manner. Here, our study provides strong evidences for the relationship of Gli1 and EMT in NSCLC.

Most of studies showed that Gli1 active through canonical Hh signaling pathway and non-cannoical Hh signaling pathway. In canonical Hh signaling pathway, Gli1 activation occurs at PTCH1 and depresses SMO. In non-canonical Hh signaling pathway, Gli1 activation did not dependent on Hh ligands and SMO[19,40,41]. And Gli1 has been demonstrated to activate non-canonically by MAPK/ERK signaling pathway, leading to tumor growth and stemness features in lung adenocarcinoma[32]. In the present study, we found that GANT-61 but not cyclopamine (SMO inhibitor) prevented EMT process in NCI-H1299 cells (Fig. 6D and Supporting Information Fig. S5). Thus, we speculate that Gli1 regulate Snail expression mainly in a non-canonical Hh Signaling pathway. And Gli1 non-canonical activation promoted Snail transcriptional activity and enhanced its protein stability. Our study provides strong evidences that non-canonical Gli1 activation is crucial for the EMT and metastasis of NSCLC. As for the underlying mechanism that mediates non-canonical Gli1 activation we will explore in the future study.

Snail, a zinc finger transcription factor, functions as an important factor for EMT and is overexpressed in many malignant tumors. Snail induces EMT process by directly inhibiting E-cadherin transcription and activating transcriptions of a series of mesenchymal genes contribute to invasive properties, leading to the enhancement of cell migration ability and tumor metastasis[42]. And elevated endogenous Snail often suggest increased metastasis potential[27,43]. Snail is an extremely unstable protein, and its protein stability is mainly regulated by ubiquitin−proteasome pathway. GSK-3β-dependent Snail phosphorylation has been recognized as a critical factor that regulating Snail degradation[44,45]. Although several researches verified that Gli1 might contribute to Snail expression in basal cell carcinoma, esophageal squamous cell cancer and esophageal adenocarcinoma. However, the underlying mechanism which Gli1 regulates Snail expression and the relationship of Gli1 and Snail in NSCLC are still largely

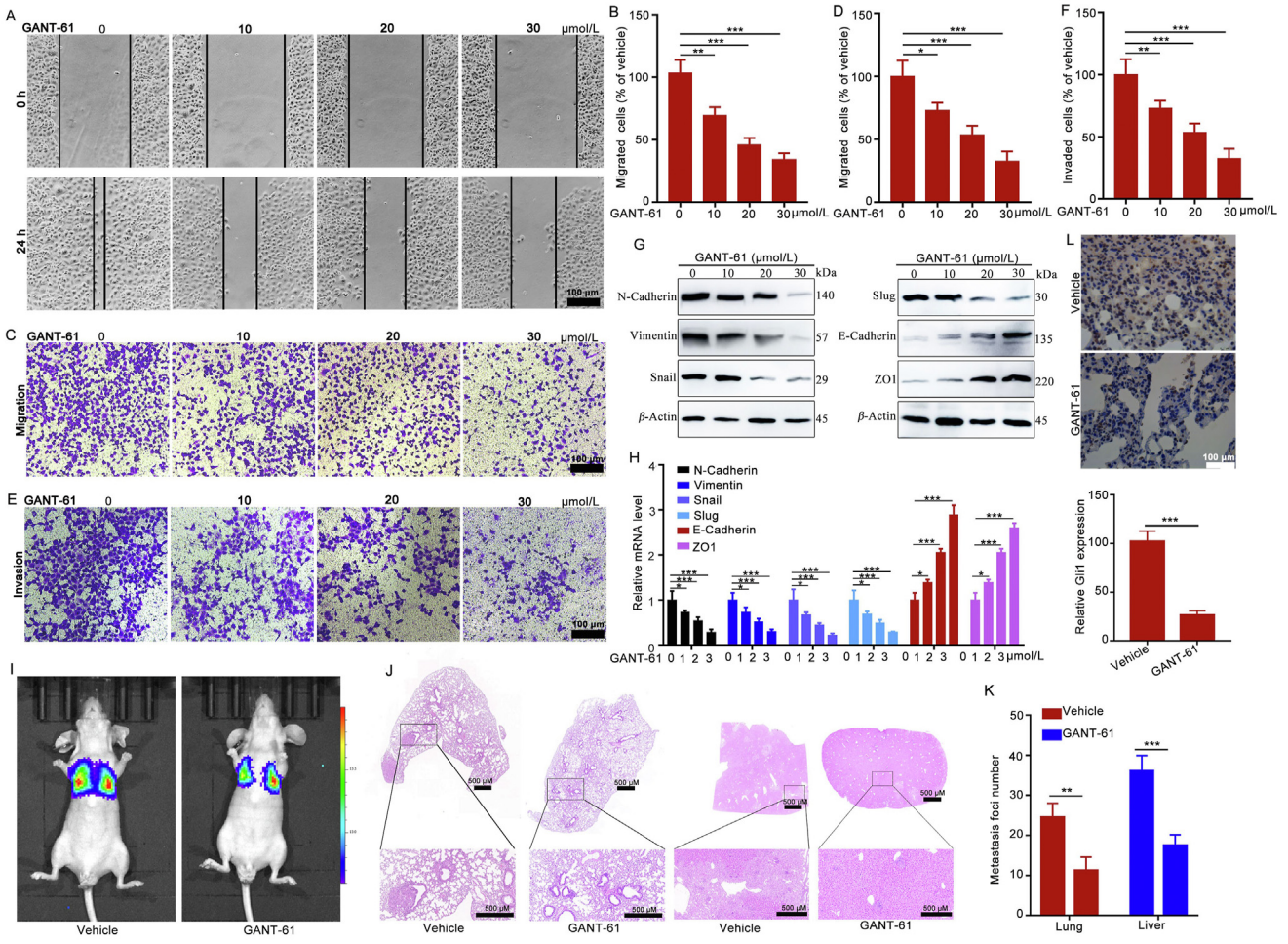

Figure 6 GANT-61 restrains the metastasis of NCI-H1299 cells *in vitro* and *in vivo*. (A−F) GANT-61 restrained the migration and invasion abilities of NCI-H1299 cells. After treated with indicated concentrations of GANT-61, NCI-H1299 cells were applied for wound healing assay (A, B), Transwell migration and invasion assay (C−F). (G, H) GANT-61 suppressed EMT of NCI-H1299 cells. The cells were treated with different concentration of GANT-61, and then the cells were collected and applied for Western blotting assay (G) and RT-qPCR assay (H) to measure the expression of several EMT markers. (I−K) GANT-61 suppressed the lung and liver metastasis of NCI-H1299 cells. NCI-H1299^{Luc} cells were intravenously injected into the mice and then intraperitoneal injected vehicle or GANT-61 (50 mg/kg) every two days for totally 30 days. IVIS Lumina II (I) and H&E staining (J) were applied to detect the nodules in the lung and liver. The statistical data of metastasis foci number in lung and liver is presented in (K). There were 10 mice in each group. Scar bar: 500 μm. (L) The Gli1 level in the lung metastasis focuses was detected by IHC assay. Representative images and quantitative data are shown. The data are presented as mean ± SD, n = three in (A)−(H), n = 10 in (I)−(L). *$P < 0.05$, **$P < 0.01$ and ***$P < 0.001$ compared with the vehicle group.

unclear[38,46,47]. Herein, we showed that Snail was associated with in Gli1-mediated enhanced effect on EMT and metastasis of NSCLC. Further research manifested that Gli1 positively regulated Snail level by promoting its transcription activity and suppressed GSK-3β-mediated Snail degradation, thereby promoting cancer invasiveness and metastasis. In addition, our study also demonstrated that Gli1 expression was positively correlated with Snail level in NSCLC patient tissues. Thus, our study provides new evidences for revealing the relationship of Gli1 and Snail in NSCLC. Our study also gives a hint for uncovering the underlying mechanism regulated Snail transcription and stability.

GANT-61 is a Gli1/Gli2 inhibitor, and has been demonstrated to restrain cell proliferation, induce cell autophagy and apoptosis in glioblastoma, cervical cancer, breast cancer[37,48,49]. Moreover, GANT-61 has been validated to attenuate TGF-beta1-mediated EMT and cell migration of A549 cells[50]. However, whether GANT-61 suppresses the invasion and metastasis of NSCLC remains largely unclear. Herein, we proved that GANT-61 restrained the migration, invasion and reversed EMT in NCI-H1299 cells. Additionally, GANT-61 administration obviously reduced metastatic foci in lung and liver. In this regard, our study gives a clue that GANT-61 may be developed into an anti-metastatic agent for NSCLC.

5. Conclusions

We demonstrated that Gli1 was a promoter of NSCLC metastasis. Further research showed that Gli1 drove NSCLC metastasis by promoting Snail transcription and enhancing its protein stability. And Gli1 overexpression indicated poor patent survival. Our study not only suggests that targeting Gli1 is a promising therapeutic approach for aggressive and metastasized NSCLC patient but also extend our understanding of the mechanisms mediated NSCLC metastasis.

Acknowledgments

This study was supported by National Natural Science Foundation of China (82104201), the GuangDong Basic and Applied Basic Research Foundation (2019A1515110058, China), the Science and Technology Program of Guangzhou (202002030026, China) and the open research funds from the Sixth Affiliated Hospital of Guangzhou Medical University, Qingyuan People's Hospital (202011-306, China) to Xueping Lei, National Natural Science Foundation of China (81903607) to Songpei Li, Research Program of Guangzhou Education Bureau (202032845, China) and the Science and Technology Program of Guangzhou (202102020017, China) to Qiudi Deng.

Author contributions

Xiyong Yu, Qiudi Deng and Zisheng Chen contributed the designed the project and revised the manuscript. Xueping Lei, Zhan Li, and Yihang Zhong performed the experiments and wrote the manuscript. Songpei Li, Jiacong Chen, Yuanyu Ke, Sha vL and Lijuan Huang analyzed data. Qianrong Pan, Lixin Zhao and Xiangyu Yang were responsible to analyzed RNA-seq data. Zisheng Chen supported clinical and pathological information.

Conflicts of interest

The authors declare no conflicts of interest.

Appendix A. Supporting information

Supporting data to this article can be found online at https://doi.org/10.1016/j.apsb.2022.05.024.

References

1. Siegel RL, Miller KD, Fuchs HE, Jemal A. Cancer statistics, 2021. *CA Cancer J Clin* 2021;**71**:7−33.
2. Ochieng JK, Kundu ST, Bajaj R, Leticia Rodriguez B, Fradette JJ, Gibbons DL. MBIP (MAP3K12 binding inhibitory protein) drives NSCLC metastasis by JNK-dependent activation of MMPs. *Oncogene* 2020;**39**:6719−32.
3. Wang Y, Wang W, Wu H, Zhou Y, Qin X, Wang Y, et al. The essential role of PRAK in tumor metastasis and its therapeutic potential. *Nat Commun* 2021;**12**:1736.
4. Herbst RS, Morgensztern D, Boshoff C. The biology and management of non-small cell lung cancer. *Nature* 2018;**553**:446−54.
5. Yuan M, Huang LL, Chen JH, Wu J, Xu Q. The emerging treatment landscape of targeted therapy in non-small-cell lung cancer. *Signal Transduct Targeted Ther* 2019;**4**:61.
6. Tian H, Lian R, Li Y, Liu C, Liang S, Li W, et al. AKT-induced lncRNA VAL promotes EMT-independent metastasis through diminishing Trim16-dependent Vimentin degradation. *Nat Commun* 2020;**11**:5127.
7. van Staalduinen J, Baker D, Ten Dijke P, van Dam H. Epithelial−mesenchymal-transition-inducing transcription factors: new targets for tackling chemoresistance in cancer?. *Oncogene* 2018;**37**:6195−211.
8. Dongre A, Weinberg RA. New insights into the mechanisms of epithelial−mesenchymal transition and implications for cancer. *Nat Rev Mol Cell Biol* 2019;**20**:69−84.
9. Yochum ZA, Cades J, Wang H, Chatterjee S, Simons BW, O'Brien JP, et al. Targeting the EMT transcription factor TWIST1 overcomes resistance to EGFR inhibitors in EGFR-mutant non-small-cell lung cancer. *Oncogene* 2019;**38**:656−70.
10. Zheng X, Dai F, Feng L, Zou H, Feng L, Xu M. Communication between epithelial−mesenchymal plasticity and cancer stem cells: new insights into cancer progression. *Front Oncol* 2021;**11**:617597.
11. Larsen JE, Nathan V, Osborne JK, Farrow RK, Deb D, Sullivan JP, et al. ZEB1 drives epithelial-to-mesenchymal transition in lung cancer. *J Clin Invest* 2016;**126**:3219−35.
12. Briscoe J, Thérond PP. The mechanisms of Hedgehog signalling and its roles in development and disease. *Nat Rev Mol Cell Biol* 2013;**14**:416−29.
13. Yang S, Liu Y, Li MY, Ng CSH, Yang SL, Wang S, et al. FOXP3 promotes tumor growth and metastasis by activating Wnt/β-catenin signaling pathway and EMT in non-small cell lung cancer. *Mol Cancer* 2017;**16**:124.
14. Deng QD, Lei XP, Zhong YH, Chen MS, Ke YY, Li Z, et al. Triptolide suppresses the growth and metastasis of non-small cell lung cancer by inhibiting β-catenin-mediated epithelial−mesenchymal transition. *Acta Pharmacol Sin* 2021;**42**:1486−97.
15. Yao Z, Han L, Chen Y, He F, Sun B, Kamar S, et al. Hedgehog signalling in the tumourigenesis and metastasis of osteosarcoma, and its potential value in the clinical therapy of osteosarcoma. *Cell Death Dis* 2018;**9**:701.
16. Amakye D, Jagani Z, Dorsch M. Unraveling the therapeutic potential of the Hedgehog pathway in cancer. *Nat Med* 2013;**19**:1410−22.
17. Sirkisoon SR, Carpenter RL, Rimkus T, Doheny D, Zhu D, Aguayo NR, et al. TGLI1 transcription factor mediates breast cancer brain metastasis *via* activating metastasis-initiating cancer stem cells and astrocytes in the tumor microenvironment. *Oncogene* 2020;**39**:64−78.
18. Wu F, Zhang Y, Sun B, McMahon AP, Wang Y. Hedgehog signaling: from basic biology to cancer therapy. *Cell Chem Biol* 2017;**24**:252−80.
19. Pietrobono S, Gagliardi S, Stecca B. Non-canonical hedgehog signaling pathway in cancer: activation of GLI transcription factors beyond smoothened. *Front Genet* 2019;**10**:556.
20. Sigafoos AN, Paradise BD, Fernandez-Zapico ME. Hedgehog/GLI signaling pathway: transduction, regulation, and implications for disease. *Cancers* 2021;**13**:3410.
21. Raz G, Allen KE, Kingsley C, Cherni I, Arora S, Watanabe A, et al. Hedgehog signaling pathway molecules and *ALDH1A1* expression in early-stage non-small cell lung cancer. *Lung Cancer* 2012;**76**:191−6.
22. Hwang J, Kang MH, Yoo YA, Quan YH, Kim HK, Oh SC, et al. The effects of sonic hedgehog signaling pathway components on non-small-cell lung cancer progression and clinical outcome. *World J Surg Oncol* 2014;**12**:268.
23. Bai XY, Zhang XC, Yang SQ, An SJ, Chen ZH, Su J, et al. Blockade of hedgehog signaling synergistically increases sensitivity to epidermal growth factor receptor tyrosine kinase inhibitors in non-small-cell lung cancer cell lines. *PLoS One* 2016;**11**:e0149370.
24. Wei C, Yang C, Wang S, Shi D, Zhang C, Lin X, et al. Crosstalk between cancer cells and tumor associated macrophages is required for mesenchymal circulating tumor cell-mediated colorectal cancer metastasis. *Mol Cancer* 2019;**18**:64.
25. Qin ZY, Wang T, Su S, Shen LT, Zhu GX, Liu Q, et al. BRD4 promotes gastric cancer progression and metastasis through acetylation-dependent stabilization of snail. *Cancer Res* 2019;**79**:4869−81.
26. Teng Y, Loveless R, Benson EM, Sun L, Shull AY, Shay C. SHOX2 cooperates with STAT3 to promote breast cancer metastasis through the transcriptional activation of WASF3. *J Exp Clin Cancer Res* 2021;**40**:274.
27. Guo X, Zhu R, Luo A, Zhou H, Ding F, Yang H, et al. EIF3H promotes aggressiveness of esophageal squamous cell carcinoma by modulating snail stability. *J Exp Clin Cancer Res* 2020;**39**:175.
28. An P, Chen F, Li Z, Ling Y, Peng Y, Zhang H, et al. HDAC8 promotes the dissemination of breast cancer cells *via* AKT/GSK-3β/Snail signals. *Oncogene* 2020;**39**:4956−69.
29. Liu Y, Zhou H, Zhu R, Ding F, Li Y, Cao X, et al. SPSB3 targets SNAIL for degradation in GSK-3β phosphorylation-dependent manner and regulates metastasis. *Oncogene* 2018;**37**:768−76.

30. Zappa C, Mousa SA. Non-small cell lung cancer: current treatment and future advances. *Transl Lung Cancer Res* 2016;**5**:288−300.
31. Kasiri S, Shao C, Chen B, Wilson AN, Yenerall P, Timmons BC, et al. GLI1 blockade potentiates the antitumor activity of PI3K antagonists in lung squamous cell carcinoma. *Cancer Res* 2017;**77**:4448−59.
32. Po A, Silvano M, Miele E, Capalbo C, Eramo A, Salvati V, et al. Noncanonical GLI1 signaling promotes stemness features and *in vivo* growth in lung adenocarcinoma. *Oncogene* 2017;**36**:4641−52.
33. Lei X, Zhong Y, Huang L, Li S, Fu J, Zhang L, et al. Identification of a novel tumor angiogenesis inhibitor targeting Shh/Gli1 signaling pathway in non-small cell lung cancer. *Cell Death Dis* 2020;**11**:232.
34. Dong H, Liu H, Zhou W, Zhang F, Li C, Chen J, et al. GLI1 activation by non-classical pathway integrin $\alpha_v\beta_3$/ERK1/2 maintains stem cell-like phenotype of multicellular aggregates in gastric cancer peritoneal metastasis. *Cell Death Dis* 2019;**10**:574.
35. Yue D, Li H, Che J, Zhang Y, Tseng HH, Jin JQ, et al. Hedgehog/Gli promotes epithelial−mesenchymal transition in lung squamous cell carcinomas. *J Exp Clin Cancer Res* 2014;**33**:34.
36. Ke B, Wang XN, Liu N, Li B, Wang XJ, Zhang RP, et al. Sonic hedgehog/Gli1 signaling pathway regulates cell migration and invasion *via* induction of epithelial-to-mesenchymal transition in gastric cancer. *J Cancer* 2020;**11**:3932−43.
37. Neelakantan D, Zhou H, Oliphant MUJ, Zhang X, Simon LM, Henke DM, et al. EMT cells increase breast cancer metastasis *via* paracrine GLI activation in neighbouring tumour cells. *Nat Commun* 2017;**8**:15773.
38. Min S, Xiaoyan X, Fanghui P, Yamei W, Xiaoli Y, Feng W. The glioma-associated oncogene homolog 1 promotes epithelial−mesenchymal transition in human esophageal squamous cell cancer by inhibiting E-cadherin *via* Snail. *Cancer Gene Ther* 2013;**20**:379−85.
39. Joost S, Almada LL, Rohnalter V, Holz PS, Vrabel AM, Fernandez-Barrena MG, et al. GLI1 inhibition promotes epithelial-to-mesenchymal transition in pancreatic cancer cells. *Cancer Res* 2012;**72**:88−99.
40. Gu D, Xie J. Non-canonical Hh signaling in cancer-current understanding and future directions. *Cancers* 2015;**7**:1684−98.
41. Pietrobono S, Gaudio E, Gagliardi S, Zitani M, Carrassa L, Migliorini F, et al. Targeting non-canonical activation of GLI1 by the SOX2−BRD4 transcriptional complex improves the efficacy of HEDGEHOG pathway inhibition in melanoma. *Oncogene* 2021;**40**:3799−814.
42. Gao J, Liu R, Feng D, Huang W, Huo M, Zhang J, et al. Snail/PRMT5/NuRD complex contributes to DNA hypermethylation in cervical cancer by TET1 inhibition. *Cell Death Differ* 2021;**28**:2818−36.
43. Jing C, Li X, Zhou M, Zhang S, Lai Q, Liu D, et al. The PSMD14 inhibitor Thiolutin as a novel therapeutic approach for esophageal squamous cell carcinoma through facilitating SNAIL degradation. *Theranostics* 2021;**11**:5847−62.
44. Ryu KJ, Park SM, Park SH, Kim IK, Han H, Kim HJ, et al. p38 stabilizes snail by suppressing DYRK2-mediated phosphorylation that is required for GSK3β-βTrCP-induced snail degradation. *Cancer Res* 2019;**79**:4135−48.
45. Zhang J, Lin X, Wu L, Huang JJ, Jiang WQ, Kipps TJ, et al. Aurora B induces epithelial−mesenchymal transition by stabilizing Snail 1 to promote basal-like breast cancer metastasis. *Oncogene* 2020;**39**:2550−67.
46. Li X, Deng W, Nail CD, Bailey SK, Kraus MH, Ruppert JM, et al. Snail induction is an early response to Gli1 that determines the efficiency of epithelial transformation. *Oncogene* 2006;**25**:609−21.
47. Wang L, Jin JQ, Zhou Y, Tian Z, Jablons DM, He B. Gli is activated and promotes epithelial−mesenchymal transition in human esophageal adenocarcinoma. *Oncotarget* 2018;**9**:853−65.
48. Carballo GB, Ribeiro JH, Lopes GPF, Ferrer VP, Dezonne RS, Pereira CM, et al. GANT-61 induces autophagy and apoptosis in glioblastoma cells despite their heterogeneity. *Cell Mol Neurobiol* 2021;**41**:1227−44.
49. Meister MT, Boedicker C, Linder B, Kögel D, Klingebiel T, Fulda S. Concomitant targeting of Hedgehog signaling and MCL-1 synergistically induces cell death in Hedgehog-driven cancer cells. *Cancer Lett* 2019;**465**:1−11.
50. Li H, Da LJ, Fan WD, Long XH, Zhang XQ. Transcription factor glioma-associated oncogene homolog 1 is required for transforming growth factor-β1-induced epithelial-mesenchymal transition of non-small cell lung cancer cells. *Mol Med Rep* 2015;**11**:3259−68.